

Chalmers Publication Library



CHALMERS

Copyright Notice IEEE

©2013 IEEE. Personal use of this material is permitted. However, permission to reprint/republish this material for advertising or promotional purposes or for creating new collective works for resale or redistribution to servers or lists, or to reuse any copyrighted component of this work in other works must be obtained from the IEEE.

(Article begins on next page)

On OTA Test in the Presence of Doppler Spreads in a Reverberation Chamber

Kristian Karlsson, *Member, IEEE*, Xiaoming Chen, Jan Carlsson, *Member, IEEE*, and Anton Skårbratt

Abstract—In this letter, over-the-air (OTA) tests of the performance of the IEEE 802.11p radio system are performed in a reverberation chamber (RC) that is equipped with a fast rotating mode stirrer. By varying the speed of the mode stirrer, different levels of Doppler spreads are created, and the 802.11p radio system is tested accordingly. As expected, the Doppler spread affects the package error rate (PER) of the radio system adversely. In addition to measurements, a simple PER model is presented, which sheds some light into the OTA tests.

Index Terms—Doppler spread, package error rate (PER), reverberation chamber (RC).

I. INTRODUCTION

REVERBERATION chambers (RCs) are traditionally used for electromagnetic compatibility (EMC) measurements. During the past decade, the RC has been successfully used in various over-the-air (OTA) tests [1]–[9]. For example, it has been used for measuring the bit error rate (BER) of certain telecommunication systems [2], [3], and the total radiated power (TRP) and the total isotropic sensitivity (TIS) of mobile terminals [4], [5]. Recently, the RC has been used to measure the throughput of a wireless local area network (WLAN) system [6] and a Long Term Evolution (LTE) system [8], [9]. Almost all the previous OTA studies were performed in RCs with negligible Doppler spread [10] (i.e., in slow-fading environments). Thus, these studies are not applicable for testing effects on wireless systems in fast-fading environments.

In this letter, an RC-based OTA testing system allowing for various Doppler spreads is presented. In order to emulate fast-fading environments, a fast-rotating mode stirrer is introduced. By changing the speed of the mode stirrer, different Doppler spreads can be generated. An 802.11p radio system (e.g., [11]) is measured in such an OTA testing system, where the package error rate (PER) is chosen to be the performance metric. Measurements show that the Doppler spread tends to reduce the effective signal-to-noise ratio (SNR) of the 802.11p radio system. Furthermore, in order to give some insight into the OTA tests, a simple PER model (based on the threshold receiver model [7] or the outage theorems [12]) is presented as well. The model can

predict the PER performance with a reasonable accuracy up to certain Doppler spread limit, above which an irreducible error floor occurs.

II. PER MODEL

PER simulations, in the literature, either deal with uncoded system, where the advanced coding that exists in modern telecommunication systems is not considered, or include specific coding at the expense of computational complexity. A simple way to include the advanced coding is to use the threshold receiver model [7], [13]. Assume that the advanced coding is powerful enough so that the receiver in an additive white Gaussian noise (AWGN) channel has a PER of zero once the received power is above a certain threshold value, and of one otherwise. Mathematically, the PER of a threshold receiver in an AWGN channel can be expressed as

$$P_e(\gamma) = \begin{cases} 1, & \gamma < \gamma_{\text{th}} \\ 0, & \gamma > \gamma_{\text{th}} \end{cases} \quad (1)$$

where γ denotes the SNR and γ_{th} represents the threshold value. In a fading environment, the average PER is

$$\overline{P_e}(\overline{\gamma}) = \int_0^{\infty} P_e(\gamma) f(\gamma; \overline{\gamma}) d\gamma \quad (2)$$

where $\overline{\gamma}$ represents the average γ and f denotes the probability density function (pdf) of γ for a given $\overline{\gamma}$. Substituting (1) into (2)

$$\overline{P_e}(\overline{\gamma}) = \int_0^{\gamma_{\text{th}}} f(\gamma; \overline{\gamma}) d\gamma = F(\gamma_{\text{th}}; \overline{\gamma}) \quad (3)$$

where F denotes the cumulative distribution function (cdf) of γ for a given $\overline{\gamma}$. The threshold receiver can be justified by the outage theorems [12], which states that, with powerful coding, the average PER can be well approximated by the outage probability of the fading channel. As a result, we will use cdf and PER interchangeably in this letter.

PER of the 802.11p radio system, which employs the orthogonal frequency-division multiplexing (OFDM) with coding and interleaving, can be easily modeled in a quasi-static channel by coherently combining the power of the independent subcarriers [7], [9]. In fast-fading environments, the Doppler spread incurs an intercarrier interference (ICI). The ICI in a 3-D isotropic scattering environment (e.g., an RC) can be readily derived by following the same lines in [14]

$$\text{ICI} = 1 - \frac{1}{N_c} \left(N_c + 2 \sum_{i=1}^{N_c-1} (N_c - i) \text{sinc}(2f_D T_s i) \right) \quad (4)$$

Manuscript received June 14, 2013; accepted July 06, 2013. Date of publication July 10, 2013; date of current version August 01, 2013.

K. Karlsson and J. Carlsson are with the Electronics Department, Technical Research Institute of Sweden, Borås 501 15, Sweden (e-mail: kristian.karlsson@sp.se).

X. Chen is with Antenna Group, Chalmers University of Technology, Gothenburg 412 96, Sweden (e-mail: xiaoming.chen@chalmers.se).

A. Skårbratt is with Bluetest AB, Gothenburg 417 55, Sweden.

Color versions of one or more of the figures in this letter are available online at <http://ieeexplore.ieee.org>.

Digital Object Identifier 10.1109/LAWP.2013.2272716

where N_c is the number of OFDM subcarriers, f_D is the maximum Doppler frequency, T_s is the sampling time, and sinc denotes the sinc function. Note that the ICI expression derived in [14] is actually for a 2-D uniform scattering environment. The extension from 2-D to 3-D isotropic environment is simply done by replacing the Bessel function with the sinc function in the ICI expression.

As explained earlier, thanks to OFDM, we can use flat-fading channel model to emulate the k th subcarrier ($k = 1, 2, \dots, N_c$)

$$y_k = H_k x_k + n_k \quad (5)$$

where x_k and y_k are transmit and receive signals, respectively, H_k denotes the channel transfer function, and n_k represents the noise (all at the k th subcarrier). In order to model the PER measured in an RC, we assume that H_k is Gaussian distributed [15]. Without loss of generality, we assume $E[|x_k|^2] = E[|n_k|^2] = 1$, where E denotes the expectation. Thus, the effective SNR at the k th subcarrier can be expressed as

$$\bar{\gamma}_k = \frac{E[|H_k|^2]}{\text{ICI}}. \quad (6)$$

The total effective SNR is

$$\bar{\gamma} = \frac{1}{N_c} \sum_{k=1}^{N_c} \bar{\gamma}_k. \quad (7)$$

Due to the Gaussian assumption of H_k , (7) is chi-square distributed [15] with $2N_i$ degrees of freedom (where N_i is the number of independent subcarrier that can be approximated as the ratio of the system bandwidth to the coherence bandwidth of the channel). Hence, the average PER becomes

$$\bar{P}_e(\bar{\gamma}) = 1 - \exp\left(-\frac{\gamma_{\text{th}} N_i}{\bar{\gamma}}\right) \sum_{l=0}^{N_i-1} \frac{1}{l!} \left(\frac{\gamma_{\text{th}} N_i}{\bar{\gamma}}\right)^l. \quad (8)$$

In general (e.g., if more complicated signal processing other than (7) is involved), a closed-form distribution of the effective SNR can be difficult to derive. Then, in simulations, we can resort to the empirical cdf

$$\bar{P}_e(\bar{\gamma}) = \frac{1}{N} \sum_{i=1}^N \mathbf{1}\{\gamma_i \leq \bar{\gamma}\} \quad (9)$$

where γ_i ($i = 1, 2, \dots, N$) are the samples of the instantaneous SNR obtained from the simulation, and the $\mathbf{1}\{\}$ denotes the indication function¹ [16]. The empirical cdf(9) is accurate with large sample number N . For simulations in Section III, we choose $N = 10\,000$, in which case, the simulated PER using (8) and (9) overlap with each other. Hence, only the simulated PERs corresponding to the empirical cdf (9) are shown in Section III.

III. MEASUREMENTS AND RESULTS

The RC-based OTA testing system (see Fig. 1) used in this work is located at SP Technical Research institute of Sweden

¹ $\mathbf{1}\{A\}$ equals 1 if the event A is true, and 0 otherwise.

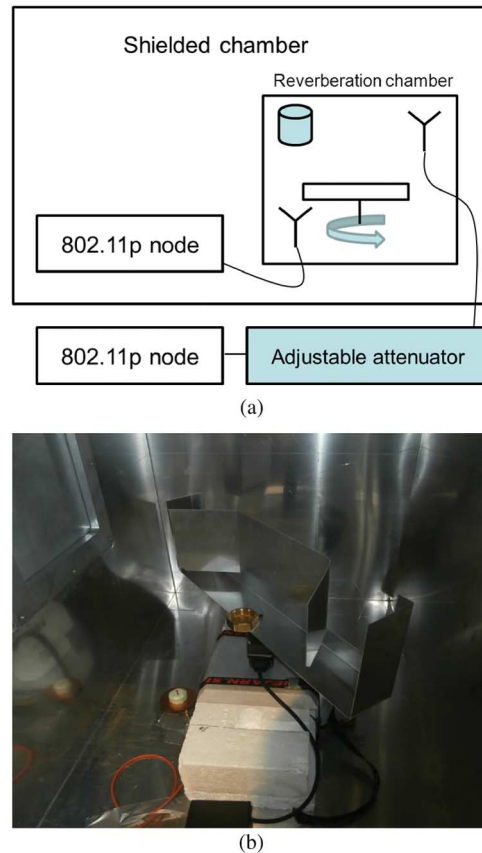


Fig. 1. (a) Illustration of the RC-based OTA testing system. (b) Photograph of the fast-rotating mode stirrer inside the RC.

(SP), Borås, Sweden. The size of the RC is $1.20 \times 1.20 \times 0.85$ m³. Both transmitter and receiver of the 802.11p radio system (based on UNEX DCMA-86P2 mini-PCI for ITS V2X applications) are placed outside the RC and are connected to external antennas located inside the RC via coaxial RF cables. High isolation is required between the radios to avoid communication directly between the radio chips. This is realized by placing one node inside a shielded chamber and the other one outside that chamber.

Measurements were performed at 5.9 GHz with 10-MHz system bandwidth and 52 OFDM subcarriers. At 5.9 GHz, the Q -factor of the RC is about 11 500, corresponding to a coherence bandwidth of about 0.5 MHz [17]. During the measurement, the mode stirrer was rotating with a controllable speed in order to emulate fast-fading environments with different Doppler spreads. We set the speed of the mode stirrer to be 1.1, 2.4, and 4.0 rounds/s (corresponding to the peripheral velocity of 2.5, 5.4, and 8.9 m/s), respectively. We denote these speeds as speed 1, speed 2, and speed 3, respectively. It was shown in [10] that the root mean square (RMS) Doppler spread in the RC can be simply approximated by v/λ , where v is the peripheral velocity of the mode stirrer and λ is the wavelength at 5.9 GHz. Thus, the RMS Doppler spreads generated by these stirrer speeds are approximately 48, 107, and 175 Hz, respectively. Note that the maximum Doppler shift frequency is larger than the RMS Doppler spread (e.g., in an ideal RC with a

constant velocity, the maximum Doppler shift is about 1.7 times larger than the RMS Doppler spread). This can be explained by the fact that the RC tends to enhance the classical Doppler shift frequency (v/λ) due to its multibounce scattering property [10]. Also note that 802.11p radio systems may encounter a larger Doppler spread. Unfortunately, due to mechanical stability, speed 3 is the upper limit of stirring speed of the mode stirrer developed in the current OTA testing system. In the future work, a faster stirrer with better mechanical stability may be implemented. Nevertheless, it should be noted that this work serves as a feasibility study of physically introducing Doppler spread into OTA tests and that the systems under test can be other systems that experience a smaller Doppler spread in practice (the 802.11p radio system is just one example of the communication systems under test).

The transmitting power of the 802.11p radio system was set to 0 dBm and package length to 30 B, including a header of approximately 20 B. Message frequency was approximately 38 Hz. In order to observe SNR dependence of the measured PERs, we use an adjustable attenuator [see Fig. 1(a)] to introduce additional path loss. The attenuator was set to have attenuations ranging from 60 to 94 dB. In addition, the cables used for the measurement introduce 11 dB insertion loss. Note that this high insertion loss is the total insertion loss in five cables used in the measurement (i.e., the cable connecting the transmit node to the connector in the wall of the RC, the cable between RC connector and the transmit antenna, the cable connecting the receive node to the connector in the wall of the shielding chamber, the cable between the connectors in the walls of the shielding chamber to the RC, respectively, and the cable from the RC connector to the receive antenna inside the RC). The five cables have a total length of about 12 m. At each attenuation value, we gathered 2000 samples, based on which the average PER was calculated. Note that the used 802.11p node (i.e., UNEX DCMA-86P2 mini-PCI) does not report noise information from the measurement. Also note that it is possible to obtain the SNR information by using the CVIS platform, e.g., [18], which estimates the SNR via the receiver signal strength indicator (RSSI). However, to date it is still a secret how the CVIS platform estimates the RSSI noise power [18]; there is no measurement verification on the estimation accuracy of the CVIS platform [19]. Thus, the SNRs reported by the CVIS platform can only be considered as relative values [18], [19]. Due to these reasons, we prefer to present the PER as a function of received power instead of SNR.

Fig. 2 shows the measured PER. As expected, by increasing the stirrer speed (and therefore the Doppler spread), the PER performance degrades. A closer look at the results reveals that the adverse effect of the Doppler spread is multifold. The Doppler spread degrades the orthogonality of the OFDM subcarriers in the 802.11p radio system. This results in an ICI, which degrades the effective SNR (represented as a shift of the PER curve to the right). In addition, the fast-fading channel makes it more difficult for channel estimation and equalization, which, once above a certain Doppler spread limit, results in an irreducible error floor, e.g., the PER corresponding to speed 3 converges to 8% at high received powers. (Note that for the sake of clear exhibition of the PER transition from 100%

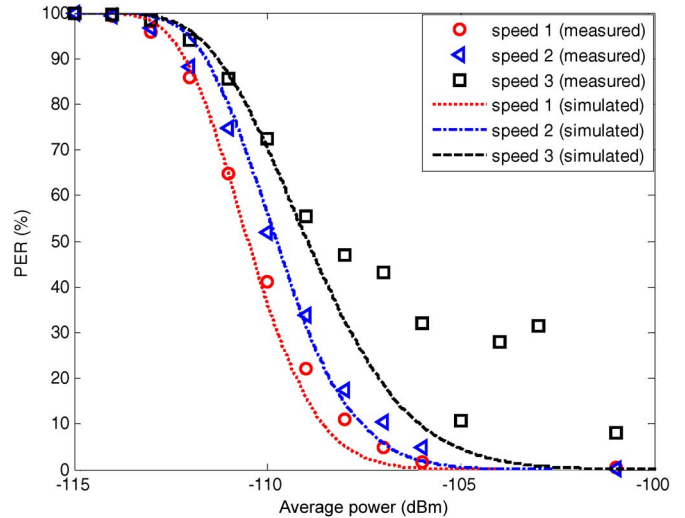


Fig. 2. Measured and simulated PER of the 802.11p radio system as a function of received power.

to 0%, the measured PER values above -100 dBm received power are not shown.) At this speed, the receiver has problems to decode messages, and many consecutive errors sometimes occur. In addition to measurements, simulated PERs (using the PER model) are also presented in Fig. 2. As can be seen, based on the threshold receiver [7] or the outage theorems [12], the modeled PER (cf. Section II) can well predict the degradation of the effective SNR due to the presence of Doppler spreads. However, the simple PER model cannot take the imperfect channel estimation and equalization into account, and therefore fails to predict the irreducible error floor at high stirrer speed.

IV. CONCLUSION

This letter focuses on the OTA tests in fast-fading environments that have been overlooked in the previous OTA studies [2]–[9]. An RC-based OTA testing system is developed. The testing system employs a fast-rotating and controllable mode stirrer inside an RC in order to emulate different Doppler spreads. To validate the developed OTA testing system, an 802.11p radio system was measured as an example. In addition to measurements, a simple PER model is presented. Measurement results show that the Doppler spread adversely affects the effective SNR of the 802.11p radio system. This phenomenon can be predicted by the PER model. However, the simple PER model fails to predict the irreducible error floor observed at high stirrer speed, which is thought to be caused by the performance degradation of the channel estimation and the equalization in the presence of large Doppler spreads.

REFERENCES

- [1] A. A. Glazunov, V. M. Kolmonen, and T. Laitinen, "MIMO over-the-air testing," in *LTE-Advanced and Next Generation Wireless Networks: Channel Modelling and Propagation*. Hoboken, NJ, USA: Wiley, 2012, pp. 411–441.
- [2] E. Genender, C. L. Holloway, K. A. Remley, J. M. Ladbury, G. Koepke, and H. Garbe, "Simulating the multipath channel with a reverberation chamber: Application to bit error rate measurements," *IEEE Trans. Electromagn. Compat.*, vol. 52, no. 4, pp. 766–777, Nov. 2010.

- [3] G. Ferrara, M. Migliaccio, and A. Sorrentino, "Characterization of GSM non-line-of-sight propagation channels generated in a reverberating chamber by using bit error rates," *IEEE Trans. Electromagn. Compat.*, vol. 49, no. 3, pp. 467–473, Aug. 2007.
- [4] C. Orlenius, P.-S. Kildal, and G. Poilasne, "Measurement of total isotropic sensitivity and average fading sensitivity of CDMA phones in reverberation chamber," in *Proc. IEEE AP-S Int. Symp.*, Washington, DC, USA, Jul. 3–8, 2005, pp. 409–412.
- [5] M. Á. García-Fernández, J. D. Sánchez-Heredia, A. M. Martínez-González, D. A. Sánchez-Hernández, and J. F. Valenzuela-Valdés, "Advances in mode-stirred reverberation chambers for wireless communication performance evaluation," *IEEE Commun. Mag.*, vol. 49, no. 7, pp. 140–147, Jul. 2011.
- [6] R. Recanatini, F. Moglie, and V. Mariani Primiani, "Performance and immunity evaluation of complete WLAN systems in a large reverberation chamber," *IEEE Trans. Electromagn. Compat.*, 2013, to be published.
- [7] P.-S. Kildal, A. Hussain, X. Chen, C. Orlenius, A. Skårbratt, J. Åsberg, T. Svensson, and T. Eriksson, "Threshold receiver model for throughput of wireless devices with MIMO and frequency diversity measured in reverberation chamber," *IEEE Antennas Wireless Propag. Lett.*, vol. 10, pp. 1201–1204, 2011.
- [8] N. Arsalane, M. Mouhamadou, C. Decroze, D. Carsenat, M. A. Garcia-Fernandez, and T. Monediere, "3GPP channel model emulation with analysis of MIMO-LTE performances in reverberation chamber," *Int. J. Antennas Propag.*, vol. 2012, p. 239420, 2012.
- [9] X. Chen, P.-S. Kildal, and M. Gustafsson, "Characterization of implemented algorithm for MIMO spatial multiplexing in reverberation chamber," *IEEE Trans. Antennas Propag.*, 2013, to be published.
- [10] K. Karlsson, X. Chen, P.-S. Kildal, and J. Carlsson, "Doppler spread in reverberation chamber predicted from measurements during step-wise stationary stirring," *IEEE Antennas Wireless Propag. Lett.*, vol. 9, pp. 497–500, 2010.
- [11] I. Ivan, P. Besnier, M. Crussière, M. Drissi, and L. Le Danvic, "Physical layer performance analysis of V2V communications in high velocity context," in *Proc. ITST*, Guyancourt, France, Oct. 20–22, 2009, pp. 409–414.
- [12] N. Prasad and M. K. Varanasi, "Outage theorems for MIMO block-fading channels," *IEEE Trans. Inf. Theory*, vol. 58, no. 7, pp. 2159–2168, Jul. 2006.
- [13] M. R. D. Rodrigues, I. Chatzigeorgiou, I. J. Wassell, and R. Carrasco, "Performance analysis of turbo codes in quasi-static fading channels," *IET Commun.*, vol. 2, no. 3, pp. 449–461, 2008.
- [14] M. Russell and G. L. Stüber, "Terrestrial digital video broadcasting for mobile reception using OFDM," *Wireless Pers. Commun.*, vol. 2, pp. 45–66, 1995.
- [15] J. G. Kostas and B. Boverie, "Statistical model for a mode-stirred chamber," *IEEE Trans. Electromagn. Compat.*, vol. 33, no. 4, pp. 366–370, Nov. 1991.
- [16] G. Grimmett and D. Stirzaker, *Probability and Random Processes*, 3rd ed. Oxford, U.K.: Oxford Univ. Press, 2001.
- [17] X. Chen, P.-S. Kildal, C. Orlenius, and J. Carlsson, "Channel sounding of loaded reverberation chamber for over-the-air testing of wireless devices—Coherence bandwidth and delay spread versus average mode bandwidth," *IEEE Antennas Wireless Propag. Lett.*, vol. 8, pp. 678–681, 2009.
- [18] A. Paier, D. Faetani, and C. F. Mecklenbräuker, "Performance evaluation of IEEE 802.11p physical layer infrastructure-to-vehicle real-world measurements," in *Proc. ISABEL*, Rome, Italy, Nov. 7–10, 2010, pp. 1–5.
- [19] S. Lin, B. Chen, and J. Lin, "Field test and performance improvement in IEEE 802.11p V2R/R2V environments," in *Proc. IEEE Int. Conf. Commun. Workshop*, Cape Town, South Africa, May 23–27, 2010, pp. 1–5.